

Modeling the mass transfer of 1,4-dioxane in a nanofiltration membrane process

Carlyn J. Higgins, Steven J. Duranceau*

University of Central Florida, Civil, Environmental, and Construction Engineering, 4000 Central Florida Boulevard, P.O. Box 162450, Orlando, FL 32816-2450, USA, Tel. +1-407-823-1440; email: steven.duranceau@ucf.edu (S.J. Duranceau), Tel. +1-407-823-6562; Fax: +1-407-823-3315; email: carlyn.higgins@knights.ucf.edu (C.J. Higgins)

Received 13 February 2020; Accepted 23 March 2020

ABSTRACT

The removal of 1,4-dioxane from groundwater was evaluated using a pilot-scale, split-feed, center-port nanofiltration (NF) process. Natural groundwater was spiked with varying concentrations of 1,4-dioxane from nanogram per liter to microgram per liter level and treated using an NF pilot process operating at a flow of 267 gpm (60,642 L/h) and 85% water recovery. The average 1,4-dioxane removal efficiency for the pilot system was 11%. Removal did not vary by solute concentration when other operating parameters (flux, temperature) were held constant. Experimentally and empirically derived 1,4-dioxane solute mass transfer coefficients were compared and inserted into diffusion-based mass transfer models such as the homogeneous solution–diffusion model (HSDM) with and without film theory (FT). The experimental and empirical solute mass transfer coefficient yielded values of 3.92 ft/d (1.38×10^{-5} m/s) and 1.60 ft/d (5.64×10^{-6} m/s), respectively. Conservative Wilke–Chang coefficients or the use of non-exact membrane dimensions may explain the difference between the experimental and empirical mass transfer coefficients. Models were ascertained for validity by comparing modeled and actual 1,4-dioxane permeate concentration via statistical analysis consisting of relative percent difference (RPD), root mean square error (RMSE), and *t*-tests. The HSDM was the most proficient at predicting 1,4-dioxane permeate concentration with an RPD of less than $\pm 8\%$ and RSME value of 0.54.

Keywords: 1,4-dioxane; Nanofiltration; Mass transfer coefficient; Homogeneous solution–diffusion model; Sherwood number; Pilot-scale

1. Introduction

The introduction of chemicals of emerging concern (CECs) into the environment is of increased cognizance due to suspected adverse ecological or human health effects from chronic exposure at the nanogram per liter (ng/L) or microgram per liter ($\mu\text{g/L}$) level [1]. One of the principal portals which CECs enter the environment is through wastewater effluent discharge, however other pathways may include poorly maintained sewers, septic tanks, landfills, and other disposal sites [2,3]. Most conventional wastewater treatment plants are not intended to remove CECs, however, some are degraded or removed in the biological treatment stage [4].

CECs have most likely been released to the environment since their introduction, but the detection of lower levels through technological advancements and newfound public awareness has sparked interest and subsequent concern [5–7]. In the United States (US), the Safe Drinking Water Act requires the Environmental Protection Agency (USEPA) to quinquennially publish a list of CECs that may potentially pose risk in drinking water, known as the Candidate Contaminant List (CCL). The CCL serves as the basis for formal monitoring programs through the Unregulated Contaminant Monitoring Rule (UCMR) which provides support regarding the regulatory process of constituents in drinking water [8].

* Corresponding author.

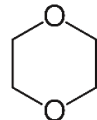
1,4-Dioxane is a heterocyclic organic CEC that has been listed on the USEPA's CCL4 and UCMR3. 1,4-Dioxane is used as an industrial solvent in adhesives, textiles, cosmetics, and dyes, and exists as a by-product of soap, polyester, and plastics manufacturing [9,10]. Detection of 1,4-dioxane in groundwater ranges from undetected to 1,000 µg/L, and up to 100,000 µg/L at some contaminated groundwater sites [10,11]. The USEPA and International Agency for Research on Cancer has classified 1,4-dioxane as a Class B2 (probable) human carcinogen due to the increased prevalence of carcinomas in rats and guinea pigs when exposed chronically to the organic compound [12,13]. Although currently unregulated, the USEPA has issued a health advisory level of 0.35 µg/L in potable water, and states within the US have set even more stringent notification levels and guidelines [14–17]. Research from the USEPA's UCMR3 suggests that 1,4-dioxane has been frequently detected in US public water supplies (PWSs), prompting the need to consider alternative treatment in response to future regulation [8].

Chemical properties of 1,4-dioxane are listed in Table 1, which highlights the mobility and persistence of 1,4-dioxane in water. A low Henry's law constant (4.8×10^{-6} atm·m³/mol) suggests that 1,4-dioxane tends to persist in aqueous environments. A low $\log K_{ow}$ (−0.27) and $\log K_{oc}$ (0.54) suggests that 1,4-dioxane is hydrophilic and does not have significant adsorptive capabilities to soil [15,18]. Hence, 1,4-dioxane is often difficult to treat from water and wastewater [13].

Conventional water treatment processes are generally ineffective at removing 1,4-dioxane [13,23–26]. However, adsorption via granular activated carbon (GAC) has shown to be moderately effective in 1,4-dioxane removal [27,28]. Regardless, GAC achieves only partial 1,4-dioxane removal, therefore other alternative treatments should be examined [13,24]. Synthetic adsorptive media, such as Ambersorb™560 manufactured by DuPont de Nemours, Inc. (Midland, MI) has displayed high removal efficiencies of 1,4-dioxane [29]. However, adsorptive media does not degrade 1,4-dioxane, which heightens concern regarding ultimate disposal. Biodegradation and advanced oxidative processes have also been investigated to remove 1,4-dioxane from aqueous sources, yielding moderate success [10,25,30–34]. Technologies are commercially available to degrade 1,4-dioxane, but high operational, electrical, and equipment replacement costs are of concern regarding applicability [13]. Other techniques such as distillation have been proven to be effective, yet energy intensive and therefore economically impracticable in most applications [23].

Prior research has examined the efficacy of membrane processes such as nanofiltration (NF) and reverse osmosis (RO) to remove CECs [3,35–38]. Existing research regarding removal of 1,4-dioxane from NF and RO is in its infant stages. Košutić et al. [39] used 1,4-dioxane as a reference solute for pore size distribution of a HR95PP RO membrane, TFC-88821ULP RO membrane, and TS80 NF membrane, and found average rejections of 92%, 88%, and 81%, respectively. In a similar study conducted by Košutić et al. [40], rejection of 1,4-dioxane for a NF270 membrane was on average 36%. Yangali-Quintanilla et al. [3] reported 1,4-dioxane rejection of 45% for a NF-90 membrane. However, rejection of CECs are dependent on solvent properties (pH, organic composition, ionic strength), solute properties (molecular weight, charge,

Table 1
Chemical properties of 1,4-dioxane

Property	Value
Structure	
CAS no.	123-91-1
Molecular weight (g/mol)	88.1
Density (g/mL)	1.033
Water solubility at 25°C (g/L)	Miscible
Boiling point (°C at 760 mmHg)	101.1
Melting point (°C)	11.8
Vapor pressure (mmHg at 25°C)	38.1
Octanol-water partition coefficient ($\log K_{ow}$)	−0.27
Soil organic carbon-water partitioning coefficient ($\log K_{oc}$)	0.54
Henry's law constant at 25°C (atm·m ³ /mol)	4.8×10^{-6}

Molecular weight and water solubility obtained from [19]; density obtained from [20], boiling point, melting point vapor pressure obtained from [21], $\log K_{ow}$, $\log K_{oc}$, Henry's law constant obtained from [22].

geometry, concentration) membrane properties (pore size, material, hydrophobicity), and process operational properties (recovery, configuration, pressure) [41–46].

Research regarding 1,4-dioxane removal has been conducted using bench-scale sized experiments and synthetic water matrices [3,23,25–28,34,40]. The objective of this work was to: determine the rejection of 1,4-dioxane in a pilot-scale NF process fed a natural groundwater matrix; model the mass transfer of 1,4-dioxane using variations of the homogeneous solution–diffusion model (HSDM); and compare the models regarding accuracy in predicting rejection of 1,4-dioxane. This work can provide valuable insight to water purveyors concerned with increasing levels of CECs such as 1,4-dioxane in their water supplies and present a model that can accurately predict its rejection in a full-scale application.

2. Mass transfer modeling

Membrane models are essential to accurately describe process behavior to minimize risk in the design of a new process or better understand how an existing process operates [47,48]. Frequently used models to predict NF and RO membrane performance consists of the Nernst–Planck equation, Kedem, and Katchalsky irreversible thermodynamic equations, Spiegler and Kedem transport equations, solution–diffusion equations, non-linear regression, among others [38,49–53]. Fundamental differences of each model are based on the mass transfer of solute, which can be described by diffusion, convection, electro-migration, or adsorption. In the solution–diffusion model, solute flux can be described based on Fick's law of diffusion, shown as Eq. (1) [54,50].

$$J_s = -D_{i,f} \frac{dC}{dx} \quad (1)$$

where J_s = solute flux (lb/ft²/d); $D_{i,f}$ = Fick's law diffusion coefficient; C = solute concentration (lb/ft³).

In the Spiegler–Kedem model, solute flux is described based on diffusion and convection, displayed as Eq. (2) [52].

$$J_s = -D_{i,f} \frac{dC}{dx} + (1 - \sigma) J_w C \quad (2)$$

where σ = reflection coefficient; J_w = water flux (gal/ft²/d).

The extended Nernst–Planck equation serves as the basis for other membrane models such as the Donnan–steric-pore-model (DSPM) and is presented as Eq. (3). The extended Nernst–Planck equation accounts for solute mass transfer due to diffusion, electro-migration, and convection [55–57].

$$J_s = -D_{i,f} \frac{dC}{dx} - \frac{z_i C D_i}{R_g T} F \frac{d\psi_d}{dx} + K_{i,c} C V \quad (3)$$

where Z_i = valence of solute; R_g = gas constant (J/mol/K); T = temperature (K); F = Faraday constant (C/mol); Ψ_d = Donnan potential difference (V); $K_{i,c}$ = hindrance factor for convection; V = solute velocity (ft/s).

Prior research has successfully used the Spiegler–Kedem equation to model rejection of salt solutions [58,59] and some uncharged organic compounds [60–62]. Similarly, the DSPM has also been used to model rejection of salts [56] and charged pharmaceuticals [57], but has over-predicted CEC rejection due to the lack of a solute-membrane partitioning consideration [63]. The DSPM has also been unsuccessful in modeling compound rejection in multi-ionic solutions [64]. In cases using low applied pressure, diffusion is the most significant rejection mechanism [55]. Moreover, 1,4-dioxane is an uncharged compound, suggesting that electrostatic interactions with the membrane surface may be negligible. Therefore, the HSDM was investigated in this work.

The HSDM was derived under the premise that solutes partition into the membrane from the feed channel, diffuse through the membrane, and partition again into the permeate stream [65]. The HSDM assumes that solvent and solute mass transfer is due to pressure and concentration gradients, respectively. Solvent mass transfer or water flux (J_w) is derived from Henry's law and Fick's first law of diffusion and is related to the water mass transfer coefficient (k_w), shown as Eq. (4). Water flux describes the amount of water treated per surface area of the membrane. Solute mass transfer or solute flux (J_s) is derived from Fick's law of diffusion under the assumption that the driving force is due to the difference in concentration, shown as Eq. (5). The solute mass transfer coefficient (k_s) can either be determined experimentally by Eq. (5), or by applying empirical analysis such as the Sherwood number correlation method (Eq. (18)).

$$J_w = k_w (\Delta P - \Delta \pi) = \frac{Q_p}{A} \quad (4)$$

$$J_s = k_s [C_m - C_p] = \frac{Q_p C_p}{A} \quad (5)$$

$$C_m = \left(\frac{C_f + C_c}{2} \right) \quad (6)$$

where k_w = water mass transfer coefficient (gal/d/ft²-psi); ΔP = transmembrane pressure (psi); $\Delta \pi$ = transmembrane osmotic pressure (psi); Q_p = permeate water flow rate (gal/d); A = effective membrane area (ft²); J_s = solute flux (lb/ft²-d); k_s = solute mass transfer coefficient (ft/d); C_p = permeate water solute concentration (lb/ft³); C_f = feed water solute concentration (lb/ft³); C_c = concentrate water solute concentration (lb/ft³); C_m = solute concentration at the membrane surface (lb/ft³).

Other pertinent equations associated with the HSDM include mass and flow balance equations around the membrane element.

$$Q_f = Q_p + Q_c \quad (7)$$

$$Q_f C_f = Q_p C_p + Q_c C_c \quad (8)$$

$$R = \left(\frac{Q_p}{Q_f} \right) \times 100 \quad (9)$$

$$r = \frac{C_f - C_p}{C_f} \times 100 \quad (10)$$

where Q_f = feedwater flow rate (gal/d); Q_c = concentrate water flow rate (gal/d); R = recovery; r = rejection.

The HSDM, shown in Eq. (11) was developed by manipulating Eqs. (4)–(10).

$$r = 1 - \frac{k_s}{k_w (\Delta P - \Delta \pi) \left(\frac{2 - 2R}{2 - R} \right) + k_s} \quad (11)$$

The HSDM can be further modified by incorporating film theory (FT), which includes effects from concentration polarization, and is known as the HSDM-FT, shown as Eq. (12).

$$r = 1 - \frac{k_s \exp\left(\frac{J_w}{k_b}\right)}{k_w (\Delta P - \Delta \pi) \left(\frac{2 - 2R}{2 - R} \right) + k_s \exp\left(\frac{J_w}{k_b}\right)} \quad (12)$$

$$\frac{C_m - C_p}{C_f - C_p} = \exp\left(\frac{J_w}{k_b}\right) \quad (13)$$

where k_b = solute back-transport mass transfer coefficient (ft/d).

The HSDM and HSDM-FT assumes a constant solute mass transfer coefficient but have incurred error due to the linear approximation of a feed concentration composition.

Therefore, an integrated HSDM and HSDM-FT were created by Mulford et al. [66] by integrating a differential equation related to instantaneous feed stream concentration into the HSDM and HSDM-FT, referred to as the IHSDM and IHSDM-FT, shown in Eqs. (14) and (15), respectively.

$$r = 1 - \frac{k_s}{-RJ_W} \ln \left(1 - \frac{RJ_W}{J_W + k_s} \right) \quad (14)$$

$$r = 1 - \frac{k_s}{-RJ_W e^{J_W/k_b}} \ln \left(1 - \frac{RJ_W}{J_W + k_s e^{J_W/k_b}} \right) \quad (15)$$

The HSDM and HSDM-FT were further modified to consider fluctuations in flux, pressure, and osmotic pressure through the membrane process, and are known as the integrated osmotic pressure model (IOPM) and integrated osmotic pressure model with film theory (IOPM-FT), displayed in Eqs. (16) and (17) [67]. Results from previous research indicate that the IOPM improved predictability of permeate concentrations when compared to the HSDM [68].

$$r = 1 - \frac{1}{R} \left\{ 1 - \left[\frac{\Delta P - k_{TDS} \times TDS_C}{\Delta P - k_{TDS} \times TDS_F} (1 - R) \right]^{\frac{k_s}{k_w \Delta P + k_s}} \right\} \quad (16)$$

$$r = 1 - \frac{1}{R} \left\{ 1 - \left(\frac{\Delta P - k_{TDS} \times TDS_C}{\Delta P - k_{TDS} \times TDS_F} \right)^{\frac{k_s}{(k_s + k_w \Delta P)}} (1 - R)^{\frac{\left[\left(\frac{J_W}{e^{J_W/k_b}} \right) k_w \Delta P \right]}{k_w \Delta P + k_s}} \right\} \quad (17)$$

where $k_{TDS} = 0.01 \text{ psi}/(\text{mg/L total dissolved solids (TDS)})$.

The HSDM model is reliant on solute flux and solute mass transfer coefficient, which are controlled by diffusion. Prior research has shown that the solute mass transfer coefficient can be determined experimentally (Eq. (5)) or by applying dimensional analysis such as the Sherwood number correlation, shown in Eq. (18) [69]. Other pertinent equations associated with the Sherwood correlation method are presented elsewhere [70]. The empirically derived solute mass transfer coefficient does not require prior operational data, which can be advantageous in modeling applications. The proposed empirical notion is supported by many researchers in finding the mass transfer coefficient, which can then be used in the HSDM or modifications of the model [38,70].

$$k_s = \frac{S_h D_i}{d_h} \quad (18)$$

where S_h = Sherwood number (dimensionless); D_i = diffusivity of solute (ft^2/s); d_h = hydraulic diameter (ft).

Diffusion-based models like the HSDM and modifications have been used in numerous membrane applications. Duranceau et al. [38] studied the removal of six synthetic organic compounds (SOCs) by NF and modeled solute mass transport by means of the HSDM. Findings include that experimental and empirical calculation of the solute mass

transfer coefficient are comparable, however empirical calculations reveal a slightly smaller mass transfer coefficient, possibly due to inaccurate membrane dimensions or conservative Wilke–Chang theoretical diffusivity. Hidalgo et al. [71] used the HSDM to model atrazine permeate concentrations of four different NF membranes, and aniline permeate concentrations from RO membranes and found that the model was accurate for low permeate atrazine concentrations. Jeffery-Black et al. [70] used the HSDM and HSDM-FT to model mass transport of caffeine through a NF membrane. Correlations of predicted vs. actual caffeine concentrations were 0.99, 0.96, and 0.99 for the HSDM, HSDM-FT, and the Sherwood-based HSDM, respectively. The HSDM-FT over predicted caffeine concentrations by 27%.

3. Materials and methods

3.1. Nanofiltration pilot unit

A 267 gallon per minute (gpm) (60,642 L/h) NF pilot located at the Town of Jupiter (Town) water utility in Florida was utilized in this research. The NF pilot is unique in that it promotes a split-feed, center port design [72]. Specifications regarding the NF pilot unit are presented in Table 2. The NF pilot unit treats a surficial groundwater supply at an average depth of 150 ft (45.7 m). Water quality of feed and permeate streams can be found in Table 4.

3.2. Experimental Procedure

Although 1,4-dioxane can be found naturally in the Town's source water ranging from non-detectable to 0.13 $\mu\text{g/L}$, a higher 1,4-dioxane concentration was needed in the feed water to effectively determine solute mass transfer and rejection. 1,4-Dioxane was purchased from Sigma Aldrich (St. Louis, MO), and injected into a feed basin containing existing pre-treated feed water. The solution was then mixed and sequentially pumped into the NF pilot unit using a 25.6 gallon per hour (gph) (96.9 L/h) positive displacement pump. Based on previous transient response work conducted on the NF pilot unit [72], 1,4-dioxane was pumped into the feed stream for at least 15 min prior to sample collection from feed, permeate, and concentrate streams. Samples were analyzed for 1,4-dioxane by EPA Method 522. The experiment was repeated eight times for a range of feed 1,4-dioxane concentrations from 170 to 38,400 ng/L , shown in Table 3. Concentrations were selected to mimic concentrations of 1,4-dioxane naturally detected in groundwater.

Water mass transfer coefficients were determined experimentally, and mass transfer coefficients were determined experimentally and empirically, then inserted into the variations of the HSDM, illustrated in Fig. 1. Experimental and theoretical outputs were compared using relative percent difference (RPD), root mean square error (RMSE), and paired t -tests.

4. Results

Feed and permeate water quality parameters were averaged over the experiments and presented in Table 4. Measurements were taken during each experiment to validate

Table 2
NF pilot unit parameters

Item	Pilot-scale value
Membrane module	8" NF270 (DOW Filmtec)
Membrane material	Polyamide thin-film composite
MWCO	300 daltons
NaCl rejection	40%–60%
Zeta potential at neutral pH	–21.6 (mV)
Number of membrane elements	54
Array	7:2
Recovery	85 (%)
Surface area per membrane	400 ft ² (37.2 m ²)
Feed capacity	267 gpm (60,642 L/h)
Production capacity	226 gpm (51,330 L/h)
Design water flux	15.1 gal/sfd (25.6 L/m ² h)
Operating feed pressure	57 psi (3.93 bar)

Membrane material, MWCO, NaCl rejection, and zeta potential obtained from [73].

Table 3
1,4-Dioxane experimental summary

Experiment no.	Feed concentration (ng/L)
1	180
2	760
3	890
4	6,200
5	15,800
6	27,000
7	37,600
8	38,400

non-fluctuation in water quality. It is important to note that the Town’s source groundwater has over 10 mg/L dissolved organic carbon (DOC) and 120 mg/L of calcium.

4.1. Determination of solute mass transfer coefficient

The solute mass transfer coefficient of 1,4-dioxane was determined experimentally and empirically. To calculate experimentally, the solute mass transfer coefficient was determined as the slope of the solute flux over the change in 1,4-dioxane concentration at the membrane surface to the total permeate stream, shown in Eq. (5). Fig. 2 illustrates the eight experimental observations plotted and the least-squares regression method to determine the average solute mass transfer coefficient value of 3.92 ft/day (1.38 × 10⁻⁵ m/s). The coefficient of determination (R²) value for the data set was 0.88, meaning the forced-fit regression line explains the

Table 4
NF pilot feed and permeate water quality

Water quality parameter	Feed water	Total permeate water
pH	6.71	6.59
Temperature (°C)	26.0	26.4
Conductivity (µS/cm)	850	540
TDS (mg/L)	590	370
Color (PtCo)	38	<5
Dissolved organic carbon (mg/L)	10.8	<0.25
Alkalinity (mg/L as CaCO ₃)	309	200
Calcium (mg/L)	121	74.2
Chloride (mg/L)	52.6	51.6
Magnesium (mg/L)	5.11	1.73
Sodium (mg/L)	22.9	19.6
Sulfate (mg/L)	68.3	1.91

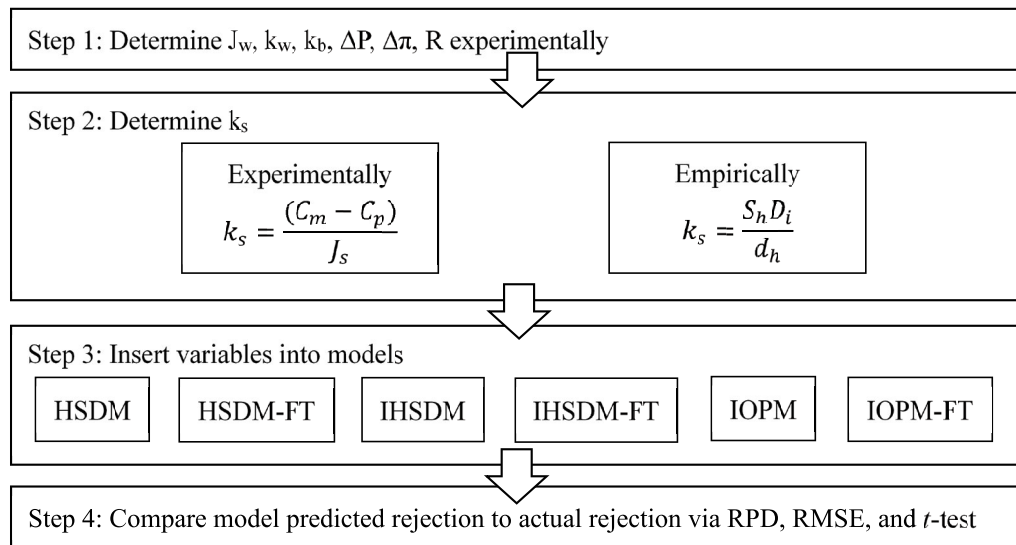


Fig. 1. Solute rejection model procedure.

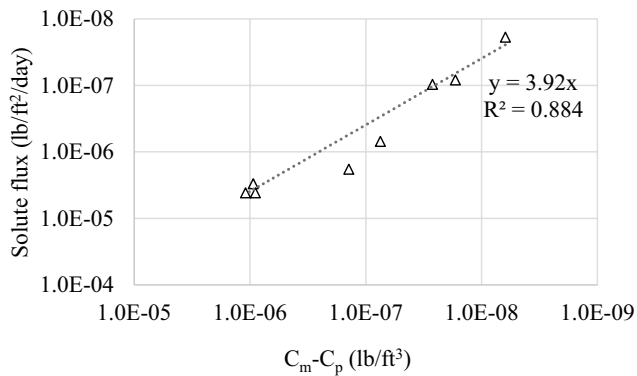


Fig. 2. 1,4-Dioxane mass transfer coefficient (presented on log-log scale).

variability for 88% of the data. The 1,4-dioxane back-transport mass transfer coefficient was also experimentally determined using Eq. (13) yielding a value of 1.79 ft/d (6.31×10^{-6} m/s) also using the least-squares regression method. The solute mass transfer coefficient of 1,4-dioxane was also calculated empirically using Sherwood relationships in accordance with Eq. (18) yielding a value of 1.60 ft/d (5.64×10^{-6} m/s). However, the empirically derived solute mass transfer coefficient (1.60 ft/d) is slightly smaller than the experimentally derived solute mass transfer coefficient (3.92 ft/d), which could be due to conservative Wilke–Chang coefficients, or non-exact dimensions of the membrane feed channel. Existing literature has realized similar results [38,70].

4.2. Determination of experimental variables

In addition to the solute mass transfer coefficient, system recovery, water flux, water mass transfer coefficient, and net driving pressure were needed to predict the rejection of 1,4-dioxane through the HSDM or its modifications. Table 5 presents a summary of the experimental values obtained from the NF pilot unit experiments.

4.3. 1,4-Dioxane rejection prediction

Average actual rejection of 1,4-dioxane was 11.7%, which is over 24% lower than the findings of Košutić et al. [40]. This difference could be due to several factors, such as the difference in membrane configuration (pilot-scale vs. flat-sheet), operational parameters (i.e., flux rate, pressure, temperature) or water matrix effects. When compared to Milli-Q water, natural water matrices have been known to decrease the rejection of CECs, specifically the presence of cations [43] or natural organic matter [74]. However, determining rejection in a pilot-scale process fed a natural water matrix may more accurately predict actual process behavior in full-scale systems.

1,4-Dioxane rejection was predicted through the HSDM and modifications (Eqs. (11), (12), (14), (15)–(17)). Average rejection percentages from each model are illustrated in Fig. 3. The average actual rejection of 1,4-dioxane was 11.7%, whereas the average HSDM predicted rejection of 1,4-dioxane was 12.5%. From Fig. 3, the HSDM-FT, IOPM, SH-HSDM-FT,

Table 5
Operational parameters taken from NF pilot

Parameter	Value
R	85 (%)
J_w	15.1 gal/ft ² /day (25.6 L/m ² h)
k_w	0.659 gal/ft ² /d-psi (2.32×10^{-6} L/m ² /h-bar)
ΔP	33.5 psi (2.31 bar)
$\Delta \pi$	10.6 psi (0.730 bar)
k_b	1.79 ft/d (6.31×10^{-6} m/s)
k_s (experimental)	3.92 ft/d (1.38×10^{-5} m/s)
k_s (empirical)	1.60 ft/d (5.64×10^{-6} m/s)

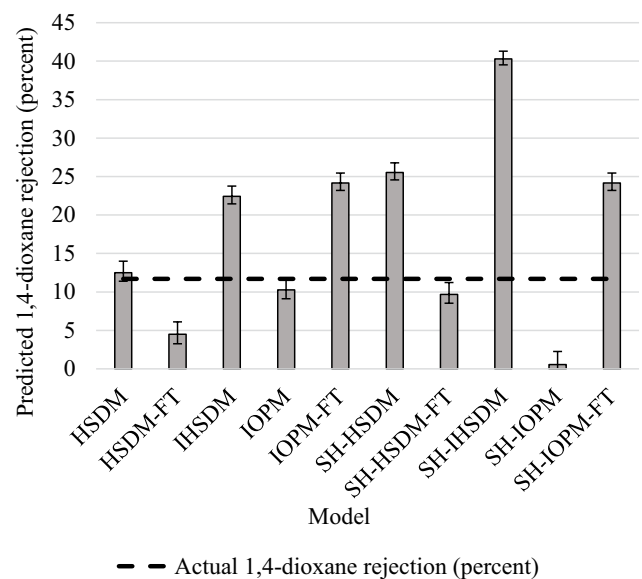


Fig. 3. Average rejections for diffusion-based models.

and SH-IOPM under-predicted 1,4-dioxane rejection, while the IHSDM, IOPM-FT, SH-HSDM, SH-IHSDM, and SH-IOPM-FT over-predicted 1,4-dioxane rejection. The IHSDM-FT and SH-IHSDM-FT severely under-predicted 1,4-dioxane permeate concentration and are thus not shown in the figure.

4.4. 1,4-Dioxane permeate concentration prediction

Using Eq. (10), the HSDM and modifications can be rearranged to solve for permeate concentration. Fig. 4 shows the actual vs. predicted 1,4-dioxane permeate concentration for the HSDM with 1,4-dioxane mass transfer coefficient calculated experimentally (HSDM) and empirically (SH-HSDM). Results are plotted on a log-log scale due to the range in 1,4-dioxane concentration. If the models predicted 1,4-dioxane permeate concentration with no error, the permeate concentrations would align with the 45° line. 1,4-Dioxane permeate concentration was predicted within $\pm 8\%$ using the HSDM but was consistently under-predicted using the SH-HSDM. As earlier mentioned, conservative Wilke–Chang coefficients or non-exact membrane dimensions may have contributed to the inaccuracy in 1,4-dioxane permeate prediction for the SH-HSDM.

Actual and model predicted permeate concentrations were compared for validity using RPD and RMSE. Fig. 5 presents the RPD range and RMSE value for the eight experiments. The HSDM, HSDM-FT, IOPM, and SH-HSDM-FT resulted in RPD values less than $\pm 10\%$ and RMSE less than 2.0. Whereas, the IHSDM, IOPM-FT, SH-HSDM, SH-IHSDM, and SH-IOPM-FT incur larger RPD and RSME values, suggesting such modifications of the HSDM should not be considered to model the rejection of 1,4-dioxane in a NF process.

In addition, a paired *t*-test with 95% confidence interval was performed to compare statistical difference between the actual and model predicted permeate concentrations. The null hypothesis tested states that the mean of the predicted permeate concentration is not significantly different than the mean of the actual permeate concentration. Table 6 displays the results from the paired *t*-test at a 95% confidence interval. The null hypothesis was not rejected for the HSDM, HSDM-FT, IOPM, and SH-HSDM-FT. Hence, the IHSDM, IHSDM-FT, IOPM-FT, SH-HSDM, SH-HSDM-FT, and SH-IOPM-FT should not be considered to accurately predict 1,4-dioxane rejection in an NF process.

Based on the average predicted rejection, RPD, RMSE, and paired *t*-test, the models best fit to predict 1,4-dioxane rejection in an NF process are: HSDM > IOPM > SH-HSDM-F

T > HSDM-FT > SH-IOPM. The results indicate the FT parameter in the model did not significantly improve 1,4-dioxane rejection prediction, suggesting negligible effects of concentration polarization on the mass transfer of 1,4-dioxane in an NF process. This could possibly be due to high water flux rate, low operational pressure, and low TDS concentration of the NF feed water, also realized by others [68,70]. The addition of an instantaneous feed parameter into the HSDM (IHSDM) decreased the accuracy of 1,4-dioxane rejection. The addition of an instantaneous flux, pressure, and osmotic pressure term in the HSDM model (IOPM) yielded similar results to the HSDM, proposing the addition of such variables had little effect in increasing the accuracy of 1,4-dioxane rejection. Further experimentation is recommended to determine best-fit predictive models for other CECs in NF processes.

5. Conclusions

In this work, the mass transfer and rejection of 1,4-dioxane were predicted using the HSDM and modifications. A 267 gpm split-feed, center-port pilot unit treating surficial groundwater was used to obtain operational parameters and conduct rejection experiments of 1,4-dioxane at concentrations ranging from 180 to 38,400 ng/L. The average actual

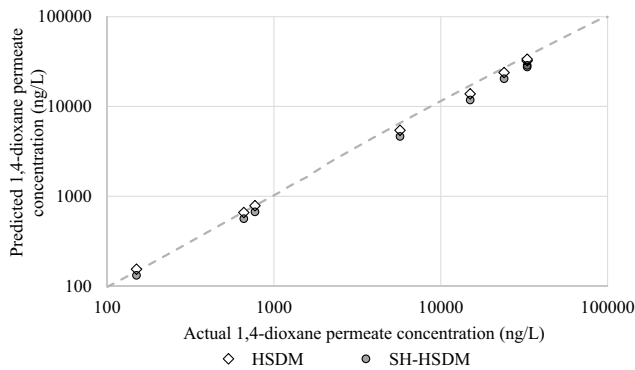


Fig. 4. Actual vs. predicted 1,4-dioxane using HSDM and SH-HSDM (presented on log–log scale).

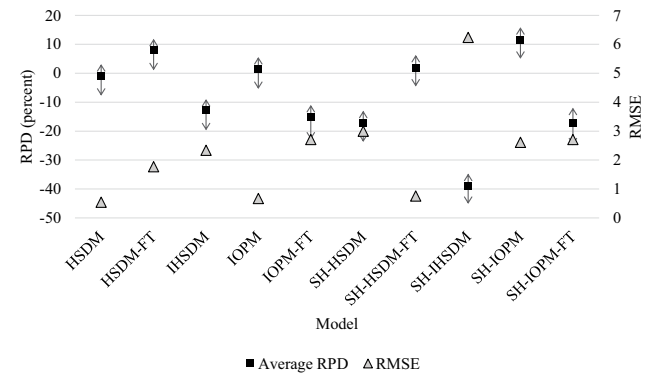


Fig. 5. RPD range and RMSE for models.

Table 6
Statistical *t*-test data

	Model	<i>t</i> -value	<i>p</i> -value	Statistically significant difference? (Y/N)
Experimental k_s	HSDM	-0.82	0.437	N
	HSDM-FT	2.14	0.070	N
	IHSDM	-2.93	0.022	Y
	IHSDM-FT	-2.77	0.027	Y
	IOPM	0.805	0.447	N
	IOPM-FT	-2.92	0.023	Y
Empirical k_s	HSDM	-2.91	0.022	Y
	HSDM-FT	1.08	0.314	N
	IHSDM	-2.84	0.025	Y
	IHSDM-FT	-2.77	0.027	Y
	IOPM	2.35	0.051	N
	IOPM-FT	-2.92	0.022	Y

rejection of 1,4-dioxane was 11%. Rejection did not vary by solute concentration when water flux and temperature were held constant.

Diffusion-based mass transfer models such as the HSDM, HSDM-FT, IHSDM, IHSDM-FT, IOPM, and IOPM-FT were assessed in this work. The 1,4-dioxane mass transfer coefficient was determined experimentally using flux relationships and empirically using Sherwood correlations and inserted into the diffusion-based models to compare rejection values. Model predicted 1,4-dioxane permeate concentration was ascertained for validity by comparing to actual 1,4-dioxane permeate concentration by means of statistical measures such as RPD, RMSE, and *t*-tests. Based on the statistical data, the models most proficient in predicting 1,4-dioxane rejection in an NF process are HSDM > IOPM > SH-HSDM-FT > HSDM-FT > SH-IOPM.

Acknowledgments

The research reported herein was funded on behalf of Jupiter Water Utilities (Jupiter, FL) through their consultant Kimley-Horn and Associates, Inc. (1920 Wekiva Way Suite 200, West Palm Beach, FL 33411) via UCF agreement 16208114. Any opinions, findings, and conclusions expressed in this material are those of the authors and do not necessarily reflect the view of UCF (Orlando, FL) or its Research Foundation. The authors acknowledge the Town of Jupiter Utilities staff, including David Brown, Amanda Barnes, Paul Jurczak, Rebecca Wilder Tony Fogel, and Gary Schulze for their assistance and support, without whom this work would not have been possible. The consultation and advice of Ian Watson (RosTek Associates Inc.) and John Potts (Kimley-Horn and Associates, Inc.) were appreciated and hereby noted. The contributions of students in the UCF Water Quality Engineering Laboratories who assisted in field and laboratory work are greatly appreciated.

Symbols

A	—	Effective membrane area, ft ²
C	—	Solute concentration, lb/ft ³
C_c	—	Concentrate water solute concentration, lb/ft ³
C_f	—	Feed water solute concentration, lb/ft ³
C_m	—	Solute concentration at the membrane surface, lb/ft ³
C_p	—	Permeate water solute concentration, lb/ft ³
D_{if}	—	Fick's law diffusion coefficient
D_i	—	Diffusivity of solute, ft ² /s
d_h	—	Hydraulic diameter, ft
F	—	Faraday constant, C/mol
J_s	—	Solute flux, lb/ft ² /d
J_w	—	Water flux, gal/ft ² /d
k_b	—	Solute back-transport mass transfer coefficient, ft/d
$K_{i,c}$	—	Hindrance factor for convection
k_w	—	Water mass transfer coefficient, gal/ft ² /d-psi
k_s	—	Solute mass transfer coefficient, ft/d
ΔP	—	Transmembrane pressure, psi
Q_f	—	Feedwater flow rate, gal/d
Q_p	—	Permeate water flow rate, gal/d
Q_c	—	Concentrate water flow rate, gal/d

r	—	Rejection, %
R	—	Recovery, %
R_g	—	Gas constant, J/mol/K
S_h	—	Sherwood number, dimensionless
T	—	Temperature, K
V	—	Solute velocity, m/s
Z_i	—	Valence of solute
$\Delta\pi$	—	Transmembrane osmotic pressure, psi
Ψ_d	—	Donnan potential difference, V
σ	—	Reflection coefficient

References

- [1] A. Kortenkamp, M. Faust, M. Scholze, T. Backhaus, Low-level exposure to multiple chemicals: reason for human health concerns?, *Environ. Health Perspect.*, 115 (2007) 106–114.
- [2] J. Fawell, C.N. Ong, Emerging contaminants and the implications for drinking water, *Int. J. Water Resour. Dev.*, 28 (2012) 247–263.
- [3] V. Yangali-Quintanilla, S.K. Maeng, T. Fujioka, M. Kennedy, G. Amy, Proposing nanofiltration as acceptable barrier for organic contaminants in water reuse, *J. Membr. Sci.*, 362 (2010) 334–345.
- [4] L.D. Nghiem, A.I. Schäfer, M. Elimelech, Pharmaceutical retention mechanisms by nanofiltration membranes, *Environ. Sci. Technol.*, 39 (2005) 7698–7705.
- [5] A.Q. Jones, C.E. Dewey, K. Doré, S.E. Majowicz, S.A. McEwen, W. David, M. Eric, D.J. Carr, S.J. Henson, Public perceptions of drinking water: a postal survey of residents with private water supplies, *BMC Public Health*, 6 (2006) 94.
- [6] F. Barbosa Jr., A. Campiglia, B. Rocha, D. Cyr, Contaminants of emerging concern: from the detection to their effects on human health, *Biomed. Res. Int.*, 2016 (2016) 1–2.
- [7] S.Y. Wee, A.Z. Aris, Occurrence and public-perceived risk of endocrine disrupting compounds in drinking water, *npj Clean Water*, 2 (2019) 1–14.
- [8] D.T. Adamson, E.A. Piña, A.E. Cartwright, S.R. Rauch, R. Hunter Anderson, T. Mohr, J.A. Connor, 1,4-Dioxane drinking water occurrence data from the third unregulated contaminant monitoring rule, *Sci. Total Environ.*, 596–597 (2017) 236–245.
- [9] A. Abe, Distribution of 1,4-dioxane in relation to possible sources in the water environment, *Sci. Total Environ.*, 227 (1999) 41–47.
- [10] R. Chen, C. Liu, N.W. Johnson, L. Zhang, S. Mahendra, Y. Liu, Y. Dong, M. Chen, Removal of 1,4-dioxane by titanium silicalite-1: separation mechanisms and bioregeneration of sorption sites, *Chem. Eng. J.*, 371 (2019) 193–202.
- [11] D.T. Adamson, S. Mahendra, K.L. Walker, S.R. Rauch, S. Sengupta, C.J. Newell, A multisite survey to identify the scale of the 1,4-dioxane problem at contaminated groundwater sites, *Environ. Sci. Technol. Lett.*, 1 (2014) 254–258.
- [12] National Toxicology Program, Bioassay of 1,4-dioxane for Possible Carcinogenicity, *Natl. Cancer Inst. Carcinog. Tech. Rep. Ser.*, 80 (1978) 1–123.
- [13] M.J. Zenker, R.C. Borden, M.A. Barlaz, Occurrence and treatment of 1,4-dioxane in aqueous environments, *Environ. Eng. Sci.*, 20 (2003) 423–432.
- [14] U.S. EPA, IRIS Toxicological Review of 1,4-Dioxane, Final Report, Washington, DC, 2010.
- [15] S. Zhang, P.B. Gedalanga, S. Mahendra, Advances in bioremediation of 1,4-dioxane-contaminated waters, *J. Environ. Manage.*, 204 (2017) 765–774.
- [16] T.K.G. Mohr, Solvent Stabilizers White Paper, Santa Clara Valley Water District, Santa Clara, CA, 2001, pp. 1–52.
- [17] A.C. McElroy, M.R. Hyman, D.R.U. Knappe, 1,4-Dioxane in drinking water: emerging for 40 years and still unregulated, *Curr. Opin. Environ. Sci. Health*, 7 (2019) 117–125.
- [18] D.K. Stepien, P. Diehl, J. Helm, A. Thoms, W. Püttmann, Fate of 1,4-dioxane in the aquatic environment: from sewage to drinking water, *Water Res.*, 48 (2014) 406–419.
- [19] S. Budavari, M.J. O'Neil, A. Smith, P. Heckelman, *The Merck Index*, Merck & Co. Inc., Rahway, NJ, 1989.

- [20] L.H. Keith, D.B. Walters, *Compendium of Safety Data Sheets for Research and Industrial Chemicals*, VCH, Deerfield Beach, FL, 1986.
- [21] K. Verschueren, *Handbook of Environmental Data on Organic Chemicals*, Van Nostrand Reinhold Co., New York, NY, 1983.
- [22] P.H. Howard, *Handbook of Environmental Fate and Exposure Data for Organic Chemicals*, Lewis Publishers, Chelsea, MI, 1989.
- [23] J.H. Suh, M. Mohseni, A study on the relationship between biodegradability enhancement and oxidation of 1,4-dioxane using ozone and hydrogen peroxide, *Water Res.*, 38 (2004) 2596–2604.
- [24] W. DiGiuseppi, C. Walecka-Hutchison, J. Hatton, 1,4-Dioxane treatment technologies, *Rem. J.*, 27 (2016) 71–92.
- [25] S. Chitra, K. Paramasivan, M. Cheralathan, P.K. Sinha, Degradation of 1,4-dioxane using advanced oxidation processes, *Environ. Sci. Pollut. Res.*, 19 (2012) 871–878.
- [26] T. Vescovi, H.M. Coleman, R. Amal, The effect of pH on UV-based advanced oxidation technologies – 1,4-Dioxane degradation, *J. Hazard. Mater.*, 182 (2010) 75–79.
- [27] M.J. McGuire, I.H. Suffet, J.V. Radziul, Assessment of unit processes for the removal of trace organic compounds from drinking water, *J. Am. Water Works Assoc.*, 70 (1978) 565–572.
- [28] M.M. Johns, W.E. Marshall, C.A. Toles, Agricultural by-products as granular activated carbons for adsorbing dissolved metals and organics, *J. Chem. Technol. Biotechnol.*, 71 (1998) 131–140.
- [29] S. Woodard, T. Mohr, M.G. Nickelsen, Synthetic media: a promising new treatment technology for 1,4-dioxane, *Rem. J.*, 24 (2014) 27–40.
- [30] C.D. Adams, P.A. Scanlan, N.D. Secrist, Oxidation and biodegradability enhancement of 1,4-dioxane using hydrogen peroxide and ozone, *Environ. Sci. Technol.*, 28 (1994) 1812–1818.
- [31] M.I. Stefan, J.R. Bolton, Mechanism of the degradation of 1,4-dioxane in dilute aqueous solution using the UV/hydrogen peroxide process, *Environ. Sci. Technol.*, 32 (1998) 1588–1595.
- [32] H.M. Coleman, V. Vimonses, G. Leslie, R. Amal, Degradation of 1,4-dioxane in water using TiO₂ based photocatalytic and H₂O₂/UV processes, *J. Hazard. Mater.*, 146 (2007) 496–501.
- [33] H. Son, J. Im, K. Zoh, A Fenton-like degradation mechanism for 1,4-dioxane using zero-valent iron (Fe⁰) and UV light, *Water Res.*, 43 (2009) 1457–1463.
- [34] V. Maurino, P. Calza, C. Minero, E. Pelizzetti, M. Vincenti, Light-assisted 1,4-dioxane degradation, *Chemosphere*, 35 (1997) 2675–2688.
- [35] B. Van der Bruggen, J. Schaep, D. Wilms, C. Vandecasteele, Influence of molecular size, polarity and charge on the retention of organic molecules by nanofiltration, *J. Membr. Sci.*, 156 (1999) 29–41.
- [36] L.D. Nghiem, T. Fujioka, *Removal of Emerging Contaminants for Water Reuse by Membrane Technology*, N.P. Hankins, R. Singh, Eds., *Emerging Membrane Technology for Sustainable Water Treatment*, Elsevier, Amsterdam, Netherlands, 2016, pp. 217–247.
- [37] B. Van der Bruggen, C. Vandecasteele, Removal of pollutants from surface water and groundwater by nanofiltration: overview of possible applications in the drinking water industry, *Environ. Pollut.*, 122 (2003) 435–445.
- [38] S.J. Duranceau, J.S. Taylor, L.A. Mulford, SOC removal in a membrane softening process, *J. Am. Water Works Assoc.*, 84 (1992) 68–78.
- [39] K. Košutić, L. Kaštelan-Kunst, B. Kunst, Porosity of some commercial reverse osmosis and nanofiltration polyamide thin-film composite membranes, *J. Membr. Sci.*, 168 (2000) 101–108.
- [40] K. Košutić, L. Furač, L. Sipoš, B. Kunst, Removal of arsenic and pesticides from drinking water by nanofiltration membranes, *Sep. Purif. Technol.*, 42 (2005) 137–144.
- [41] S. Darvishmanesh, J. Degrève, B. Van der Bruggen, Mechanisms of solute rejection in solvent resistant nanofiltration: the effect of solvent on solute rejection, *Phys. Chem. Chem. Phys.*, 12 (2010) 13333–13342.
- [42] T.-J. Liu, E.-E. Chang, P.-C. Chiang, Effects of concentrations and types of natural organic matters on rejection of compounds of emerging concern by nanofiltration, *Desal. Water Treat.*, 51 (2013) 6929–6939.
- [43] A.M. Comerton, R.C. Andrews, D.M. Bagley, The influence of natural organic matter and cations on the rejection of endocrine disrupting and pharmaceutically active compounds by nanofiltration, *Water Res.*, 43 (2009) 613–622.
- [44] C.Y. Tang, S. Fu, C.S. Criddle, J.O. Leckie, Effect of flux (transmembrane pressure) and membrane properties on fouling and rejection of reverse osmosis and nanofiltration membranes treating perfluorooctane sulfonate containing wastewater, *Environ. Sci. Technol.*, 41 (2007) 2008–2014.
- [45] E. Steinle-Darling, M. Reinhard, Nanofiltration for trace organic contaminant removal: structure, solution, and membrane fouling effects on the rejection of perfluorochemicals, *Environ. Sci. Technol.*, 42 (2008) 5292–5297.
- [46] C. Bellona, J.E. Drewes, P. Xu, G. Amy, Factors affecting the rejection of organic solutes during NF/RO treatment—a literature review, *Water Res.*, 38 (2004) 2795–2809.
- [47] J. Marriott, E. Sørensen, A general approach to modelling membrane modules, *Chem. Eng. Sci.*, 58 (2003) 4975–4990.
- [48] Y. Zhao, J.S. Taylor, S. Chellam, Predicting RO/NF water quality by modified solution diffusion model and artificial neural networks, *J. Membr. Sci.*, 263 (2005) 38–46.
- [49] R. Schlögl, Membrane permeation in systems far from equilibrium, *Ber. Bunsen Ges. Phys. Chem.*, 70 (2010) 400–414.
- [50] J.G. Wijmans, R.W. Baker, The solution-diffusion model: a review, *J. Membr. Sci.*, 107 (1995) 1–21.
- [51] O. Kedem, A. Katchalsky, Thermodynamic analysis of the permeability of biological membranes to non-electrolytes, *Biochim. Biophys. Acta*, 27 (1958) 229–246.
- [52] K.S. Spiegler, O. Kedem, Thermodynamics of hyperfiltration (reverse osmosis): criteria for efficient membranes, *Desalination*, 1 (1966) 311–326.
- [53] W.R. Bowen, A.W. Mohammad, N. Hilal, Characterisation of nanofiltration membranes for predictive purposes – use of salts, uncharged solutes and atomic force microscopy, *J. Membr. Sci.*, 126 (1997) 91–105.
- [54] H.K. Lonsdale, U. Merten, R.L. Riley, Transport properties of cellulose acetate osmotic membranes, *J. Appl. Polym. Sci.*, 9 (1965) 1341–1362.
- [55] W.R. Bowen, A.W. Mohammad, Characterization and prediction of nanofiltration membrane performance—a general assessment, *Chem. Eng. Res. Des.*, 76 (1998) 885–893.
- [56] A.W. Mohammad, N. Hilal, H. Al-Zoubi, N.A. Darwish, Prediction of permeate fluxes and rejections of highly concentrated salts in nanofiltration membranes, *J. Membr. Sci.*, 289 (2007) 40–50.
- [57] A.D. Shah, C. Huang, J. Kim, Mechanisms of antibiotic removal by nanofiltration membranes: model development and application, *J. Membr. Sci.*, 389 (2012) 234–244.
- [58] H. Al-Zoubi, N. Hilal, N.A. Darwish, A.W. Mohammad, Rejection and modelling of sulphate and potassium salts by nanofiltration membranes: neural network and Spiegler–Kedem model, *Desalination*, 206 (2007) 42–60.
- [59] S. Koter, Determination of the parameters of the Spiegler–Kedem–Katchalsky model for nanofiltration of single electrolyte solutions, *Desalination*, 198 (2006) 335–345.
- [60] A.M. Hidalgo, G. León, M. Gómez, M.D. Murcia, E. Gómez, J.L. Gómez, Application of the Spiegler–Kedem–Kachalsky model to the removal of 4-chlorophenol by different nanofiltration membranes, *Desalination*, 315 (2013) 70–75.
- [61] J.L.C. Santos, P. de Beukelaar, I.F.J. Vankelecom, S. Velizarov, J.G. Crespo, Effect of solute geometry and orientation on the rejection of uncharged compounds by nanofiltration, *Sep. Purif. Technol.*, 50 (2006) 122–131.
- [62] A.R.D. Verliefde, E.R. Cornelissen, S.G.J. Heijman, Verberk, J.Q.J.C. Verberk, G.L. Amy, B. Van der Bruggen, J.C. van Dijk, Construction and validation of a full-scale model for rejection of organic micropollutants by NF membranes, *J. Membr. Sci.*, 339 (2009) 10–20.
- [63] X. Wang, B. Li, T. Zhang, X. Li, Performance of nanofiltration membrane in rejecting trace organic compounds: experiment and model prediction, *Desalination*, 370 (2015) 7–16.

- [64] O. Labban, C. Liu, T.H. Chong, J.H. Lienhard V, Fundamentals of low-pressure nanofiltration: membrane characterization, modeling, and understanding the multi-ionic interactions in water softening, *J. Membr. Sci.*, 521 (2017) 18–32.
- [65] J. Wang, D.S. Dlamini, A.K. Mishra, M.T.M. Pendergast, M.C.Y. Wong, B.B. Mamba, V. Freger, A.R.D. Verliefdee, E.M.V. Hoek, A critical review of transport through osmotic membranes, *J. Membr. Sci.*, 454 (2014) 516–537.
- [66] L.A. Mulford, J.S. Taylor, D.M. Nickerson, S.S. Chen, NF performance at full and pilot scale, *J. Am. Water Works Assoc.*, 91 (1999) 64–75.
- [67] Y. Zhao, Modeling of Membrane Solute Mass Transfer in NF/RO Membrane Systems, University of Central Florida, 2004.
- [68] Y. Zhao, J.S. Taylor, Incorporation of osmotic pressure in an integrated incremental model for predicting RO or NF permeate concentration, *Desalination*, 174 (2005) 145–159.
- [69] T.K. Sherwood, P.L.T. Brian, R.E. Fisher, Desalination by reverse osmosis, *Ind. Eng. Chem. Fundam.*, 6 (1967) 2–12.
- [70] S. Jeffery-Black, S.J. Duranceau, C. Franco, Caffeine removal and mass transfer in a nanofiltration membrane process, *Desal. Water Treat.*, 59 (2017) 1–10.
- [71] A.M. Hidalgo, G. León, M. Gómez, M.D. Murcia, D.S. Barbosa, P. Blanco, Application of the solution-diffusion model for the removal of atrazine using a nanofiltration membrane, *Desal. Water. Treat.*, 51 (2013) 2244–2252.
- [72] S. Jeffery-Black, S.J. Duranceau, Mass transfer and transient response time of a split-feed nanofiltration pilot unit, *Desal. Water Treat.*, 57 (2016) 25388–25398.
- [73] M.J. López-Muñoz, A. Sotto, J.M. Arsuaga, B. Van der Bruggen, Influence of membrane, solute and solution properties on the retention of phenolic compounds in aqueous solution by nanofiltration membranes, *Sep. Purif. Technol.*, 66 (2009) 194–201.
- [74] X. Jin, J. Hu, S.L. Ong, Removal of natural hormone estrone from secondary effluents using nanofiltration and reverse osmosis, *Water Res.*, 44 (2010) 638–648.